# Modulation of the cellular organelle specificity in Re(I) tetrazolato complexes leads to unprecedented phosphorescent labeling of lipid droplets

Christie A. Bader,[a] Robert D. Brooks,[a] Yeap S. Ng,[a] Alexandra Sorvina,[a] Melissa V. Werrett,[b] Phillip J. Wright,[b] Ayad G. Anwer,[c] Douglas A. Brooks,[a] Stefano Stagni,[d] Sara Muzzioli,[d] Morry Silberstein,[b] Brian W. Skelton,[e] Ewa M. Goldys,[c] Sally E. Plush,[a] Tetyana Shandala,*[,a] Massimiliano Massi*[,b]

[a] *School of Pharmacy and Medical Science, University of South Australia, Adelaide 5001 SA, Australia*

[b] *Department of Chemistry, Curtin University, Bentley 6102 WA, Australia*

[c] *Department of Physics and Astronomy, Macquarie University, North Ryde 2109 NSW, Australia*

[d] *Department of Industrial Chemistry, University of Bologna, Bologna 40126, Italy*

[e] *Centre for Microscopy, Characterisation and Analysis, University of Western Australia, Crawley 6009 WA, Australia*

Corresponding author Email: Tetyana.Shandala@unisa.edu.au; M.Massi@curtin.edu.au.

**Electronic Supplementary Information**

**General Considerations**

All the reagents and solvents were obtained from Sigma Aldrich and used as received without any further purification. Complex **1** was prepared according to a previously published procedure.[1] Although not strictly required, all the reactions involving the Re complexes were carried out under a nitrogen atmosphere following Schlenk protocols. IR spectra were recorded on solid samples using a diamond ATR Perkin-Elmer Spectrum 100 FT-IR. Nuclear magnetic resonance spectra (consisting of $^{1}H$ and $^{13}C$) were recorded using a Bruker Avance 400 spectrometer (400.1 MHz for $^{1}H$, 100 MHz for $^{13}C$) at room temperature. $^{1}H$ and $^{13}C$ chemical shifts were referenced to residual solvent resonances. Elemental analyses were performed by the Central Science Laboratory (University of Tasmania) on the bulk samples.

**Photophysical Measurements**

Absorption spectra were recorded at room temperature using a Cary 4000 UV/Vis spectrometer. Uncorrected steady state emission and excitation spectra were recorded on an Edinburgh FLSP980-S2S2-stm spectrometer equipped with: i) a temperature-monitored cuvette holder; ii) 450 W Xenon arc lamp; iii) double excitation and emission monochromators; iv) a Peltier cooled Hamamatsu R928P photomultiplier tube (spectral range 200-870 nm). Emission and excitation spectra were corrected for source intensity (lamp and grating) and emission spectral response (detector and grating) by a calibration curve supplied with the instrument. According to the approach described by Demas and Crosby,[2] luminescence quantum yields ($\Phi_{em}$) were measured in optically dilute solutions (O.D. < 0.1 at excitation wavelength) obtained from absorption spectra on a wavelength scale [nm] and compared to the reference emitter by the following equation:

$$\Phi_x = \Phi_r \left[\frac{A_r(\lambda_r)}{A_x(\lambda_x)}\right]\left[\frac{I_r(\lambda_r)}{I_x(\lambda_x)}\right]\left[\frac{n_x^2}{n_r^2}\right]\left[\frac{D_x}{D_r}\right]$$

where $A$ is the absorbance at the excitation wavelength ($\lambda$), $I$ is the intensity of the excitation light at the excitation wavelength ($\lambda$), $n$ is the refractive index of the solvent, $D$ is the integrated intensity of the luminescence and $\Phi$ is the quantum yield. The subscripts $r$ and $x$ refer to the reference and the sample, respectively. The quantum yield determinations were performed at identical excitation wavelength for the sample and the reference, therefore cancelling the $I(\lambda_r)/I(\lambda_x)$ term in the

equation. The quantum yields of complexes **1** and **2** were measured against an air-equilibrated 0.1 M $H_2SO_4$ solution of quinine sulfate ($\Phi_r$ = 0.53).[3] Emission lifetimes ($\tau$) were determined with the time correlated single photon counting technique (TCSPC) with the same Edinburgh FLSP980-S2S2-stm spectrometer using pulsed picosecond LEDs (EPLED/EPL 377nm, FHWM < 800 ps). The goodness of fit was assessed by minimizing the reduced $\chi^2$ function and by visual inspection of the weighted residuals. The solvents (dichloromethane and a solution of $H_2O$:DMSO (99:1) used for the preparation of the solutions for the photophysical investigations were of LR grade and the water was deionized. Experimental uncertainties are estimated to be ±8% for lifetime determinations, ±20% for quantum yields, ±2 nm and ±5 nm for absorption and emission peaks, respectively.

**Synthetic Details**

**Synthesis of 2**

*fac*-[Re(CO)$_3$(**phen**)Cl],[4] **phen** = 1,10-phenanthroline, and 3-(1H-tetrazol-5-yl)pyridine[5] were prepared according to previously published methods. To a suspension of *fac*-[Re(CO)$_3$(**phen**)Cl] (0.1 g, 0.2 mmol) in acetonitrile, 2 eq. of 3-(1H-tetrazol-5-yl)pyridine and 2 eq. of triethylamine were added. The resulting suspension was heated at reflux for 72 hours. The solvent was removed and the residual yellow solid was purified via column chromatography with the use of basic alumina as the stationary phase (Brockmann activity II) and an acetonitrile solution containing 5% methanol. After the elution of a first fraction identified as unreacted starting material *fac*-[Re(CO)$_3$(**phen**)Cl], the second fraction was collected and reprecipitated from a DCM solution by addition of diethyl ether. Yield: 0.062 g (49%). Mp: 250 ˚C (dec.). Elemental analysis for $C_{21}H_{12}N_7O_3Re•H_2O$: calcd: C 41.04, H 2.30, N 15.95; found: C 41.36, H 2.00 N 16.02 (a corresponding water peak was visible also in the $^1$H-NMR spectrum). IR ($\nu$, cm$^{-1}$): 2017 s (CO, A'(1)), 1883 s br (CO, A'(2)/A''). $^1$H NMR (δ, ppm, $CDCl_3$): 9.54 (2H, d, $J$ = 5.2 Hz: **phen** H2, H9), 8.83 (1H, s: py H2), 8.57 (2H, d, $J$ = 8.2 Hz: **phen** H4, H7), 8.43 (1H, d, $J$ = 4.8 Hz: py H6), 8.10 (1H, d, $J$ = 8.3 Hz: py H4), 8.01 (2H, s: **phen** H5, H6), 7.92-7.88 (2H, m: **phen** H3, H8), 7.20-7.16 (1H, m: py H5). $^{13}$C NMR (δ, ppm, $CDCl_3$): 196.6 (CO), 193.7 (CO), 161.1 ($\underline{C}N_4$), 153.9, 149.3, 147.8, 147.7, 138.6, 133.6, 130.6, 127.7, 126.1, 126.0, 123.4.

**X-ray Crystal Diffraction Studies**

Crystallographic data for the structures were collected at 100(2) K on an Oxford Diffraction Gemini diffractometer fitted with Mo Kα radiation. Following analytical absorption corrections and solution by direct methods, the structure was refined against $F^2$ with full-matrix least-squares using the program SHELXL-97.[6] The pyridyltetrazole ligand is disordered over two sets of sites with occupancy factors refined to 0.606(2) and its complement. Anisotropic displacement parameters were employed for the non-hydrogen atoms. All H-atoms were added at calculated positions and refined by use of a riding model with isotropic displacement parameters based on those of the parent atom. Full details of the structure determination (except structure factors) have been deposited with the Cambridge Crystallographic Data Centre as CCDC 974717. Copies of this information may be obtained free of charge from The Director, CCDC, 12 Union Road, Cambridge CB2 1EZ, UK (Fax: + 44 1223 336 033; e-mail: deposit@ccdc.cam.ac.uk or www: http://www.ccdc.cam.ac.uk).

**Table S1**. Crystal data and structure refinement for **2**.

| | |
|---|---|
| Empirical formula | $C_{21}H_{12}N_7O_3Re$ |
| Formula weight | 596.58 |
| Temperature | 100(2) K |
| Wavelength | 0.71073 Å |
| Crystal system | Monoclinic |
| Space group | $P2_1/c$ |
| Unit cell dimensions | $a$ = 6.78040(10) Å |
| | $b$ = 16.5729(4) Å |
| | $c$ = 17.5034(4) Å |
| | β= 92.688(2)° |
| Volume | 1964.71(7) $Å^3$ |
| Z | 4 |
| Density (calculated) | 2.017 $Mg/m^3$ |
| Absorption coefficient | 6.227 $mm^{-1}$ |
| Crystal size | 0.47 x 0.09 x 0.05 $mm^3$ |
| θ range for data collection | 3.71 to 38.00°. |

| | |
|---|---|
| Index ranges | -11<=h<=11, -28<=k<=28, -30<=l<=30 |
| Reflections collected | 63582 |
| Independent reflections | 10677 [R(int) = 0.0645] |
| Completeness to θ = 38.00° | 99.8 % |
| Absorption correction | Analytical |
| Max. and min. transmission | 0.834 and 0.282 |
| Refinement method | Full-matrix least-squares on $F^2$ |
| Data / restraints / parameters | 10677 / 6 / 389 |
| Goodness-of-fit on $F^2$ | 0.794 |
| Final R indices [$I$>2σ($I$)] | $R1$ = 0.0277, $wR2$ = 0.0397 |
| R indices (all data) | $R1$ = 0.0602, $wR2$ = 0.0422 |
| Largest diff. peak and hole | 2.007 and -2.172 e.Å$^{-3}$ |

**Table S2**. Selected bond lengths [Å] and angles [°] for **2**.

| | |
|---|---|
| Re(1)-C(3) | 1.917(2) |
| Re(1)-C(2) | 1.918(2) |
| Re(1)-C(1) | 1.922(2) |
| Re(1)-N(2') | 2.036(6) |
| Re(1)-N(11) | 2.1680(15) |
| Re(1)-N(21) | 2.1745(16) |
| Re(1)-N(2) | 2.251(4) |
| | |
| C(3)-Re(1)-C(2) | 90.46(9) |
| C(3)-Re(1)-C(1) | 89.52(9) |
| C(2)-Re(1)-C(1) | 88.39(11) |
| C(3)-Re(1)-N(2') | 90.06(19) |
| C(2)-Re(1)-N(2') | 171.81(14) |
| C(1)-Re(1)-N(2') | 83.45(15) |
| C(3)-Re(1)-N(11) | 95.72(7) |
| C(2)-Re(1)-N(11) | 96.18(7) |

| | |
|---|---|
| C(1)-Re(1)-N(11) | 173.01(9) |
| N(2')-Re(1)-N(11) | 91.90(13) |
| C(3)-Re(1)-N(21) | 169.72(7) |
| C(2)-Re(1)-N(21) | 96.21(7) |
| C(1)-Re(1)-N(21) | 98.46(8) |
| N(2')-Re(1)-N(21) | 84.45(18) |
| N(11)-Re(1)-N(21) | 75.83(6) |
| C(3)-Re(1)-N(2) | 92.06(12) |
| C(2)-Re(1)-N(2) | 174.96(11) |
| C(1)-Re(1)-N(2) | 96.00(12) |
| N(11)-Re(1)-N(2) | 79.23(9) |
| N(21)-Re(1)-N(2) | 80.72(11) |

**Photophysical Properties**

**Table S1**. Summary of the photophysical data of complex **1** and **2** in air-equilibrated diluted $H_2O$:DMSO (99:1) and DCM.

| Complex | ($H_2O$:DMSO) (99:1) | | | | Dichloromethane | | | |
|---|---|---|---|---|---|---|---|---|
| | $\lambda_{abs}$ (nm) $10^4\varepsilon$ (L mol$^{-1}$ cm$^{-1}$) | $\lambda_{em}$ (nm) | $\tau$ (ns) | $\Phi$ | $\lambda_{abs}$ (nm) $10^4\varepsilon$ (L mol$^{-1}$ cm$^{-1}$) | $\lambda_{em}$ (nm) | $\tau$ (ns) | $\Phi$ |
| **1 ($10^{-5}$ M)** | 266 (8.6)<br>378 (0.54) | 569 | 575 (14%)<br>2373 (86%) | 0.103 | 275 (4.51)<br>366 (0.46) | 585 | 303 | 0.041 |
| **1 ($10^{-6}$ M)** | | 583 | 279 | | | 586 | 301 | |
| **2 ($10^{-5}$ M)** | 266 (8.37)<br>370 (0.34) | 582 | 277 | 0.018 | 261 (3.57)<br>362 (0.41) | 587 | 279 | 0.036 |
| **2 ($10^{-6}$ M)** | | 581 | 271 | | | 581 | 278 | |

The photophysical results show that the excited state lifetime and quantum yield values of **1** in a $10^{-5}$ M $H_2O$:DMSO 99:1 solution are significantly increased compared to the measurements in DCM at the same concentration. The emission is also slightly blue shifted. On the other hand, there is substantially no difference between the two solutions of **2** in dichloromethane and water. To try and explain the behavior of complex **1**, the photophysical data were also obtained from solution with a concentration of *ca.* $10^{-6}$ M, where both complexes **1** and **2** have similar properties in either $H_2O$:DMSO 99:1 or DCM. These results may suggest that complex **1** in $H_2O$:DMSO starts aggregating at a concentration of $10^{-5}$ M. Measurement of **1** in the solid state in fact shows a blue shifted emission at 532 nm. The lifetime of **2** in the solid state is biexponential with a 2030 ns component (69%) and a 900.27 ns component (31%). The long lifetime seen in the solid state is of the same order of magnitude as that of **1** in $H_2O$:DMSO. These solid state photophysical measurements support the argument for potential aggregation of **1** in the aqueous solution.

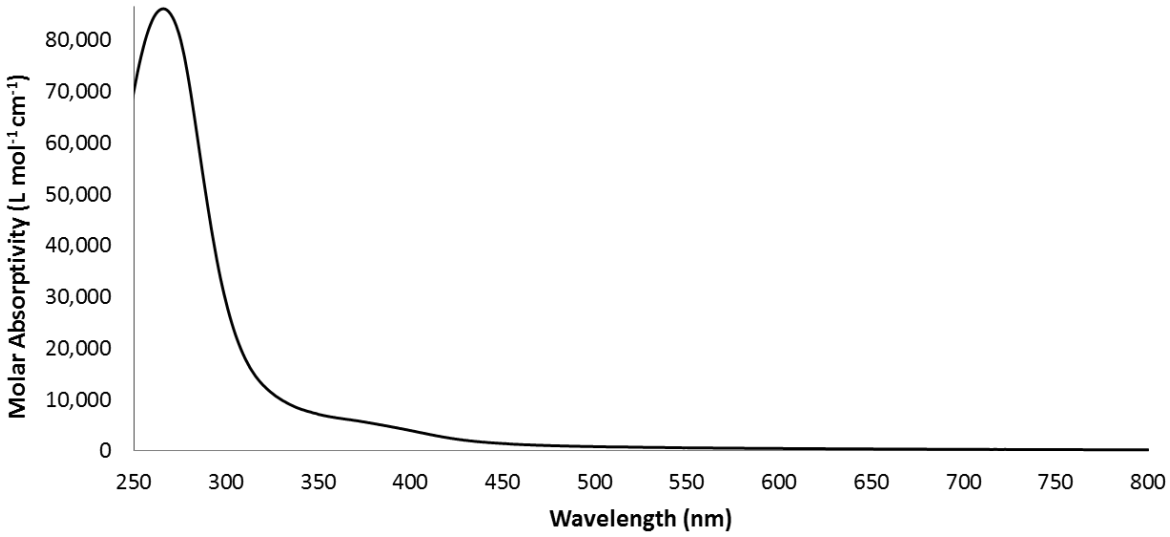


**Figure S1**. Absorption of **1** ($10^{-5}$ M) in $H_2O$:DMSO (99:1).

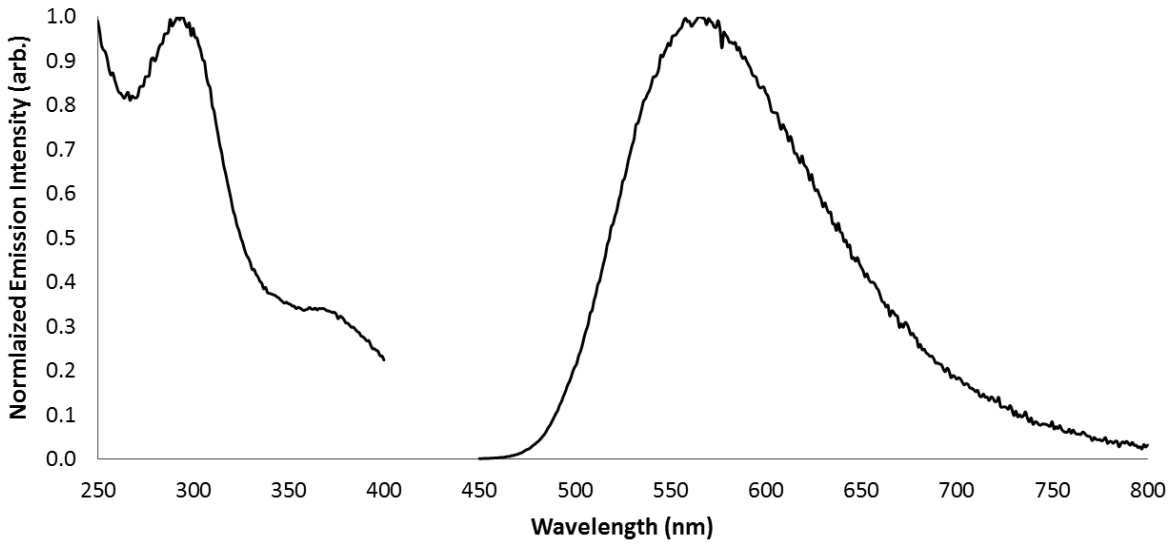


**Figure S2**. Normalised excitation and emission of **1** ($10^{-5}$ M) in $H_2O$:DMSO (99:1).

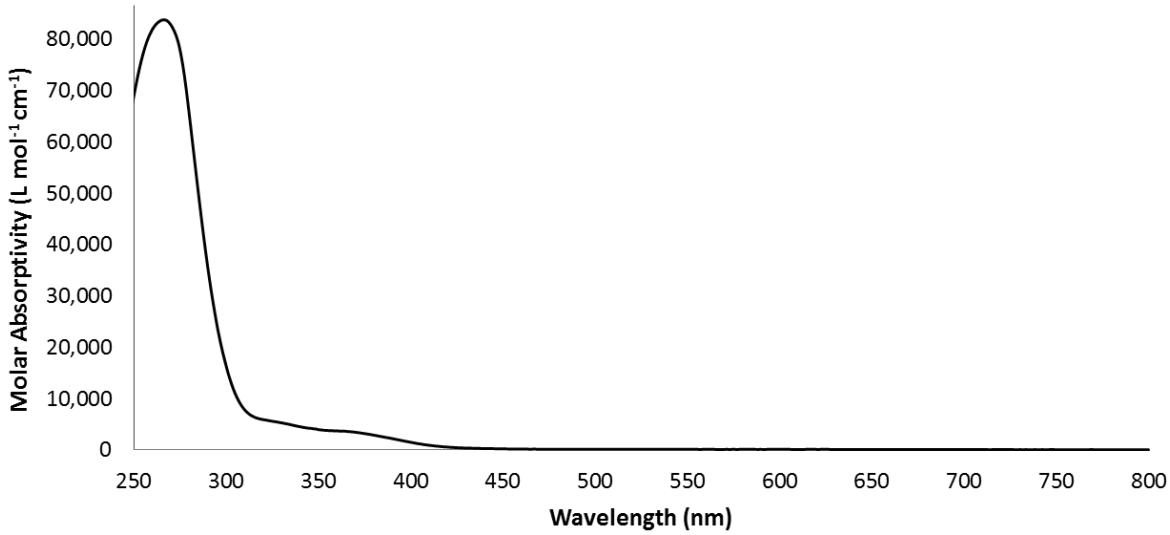


**Figure S3**. Absorption of **2** ($10^{-5}$ M) in $H_2O$:DMSO (99:1).

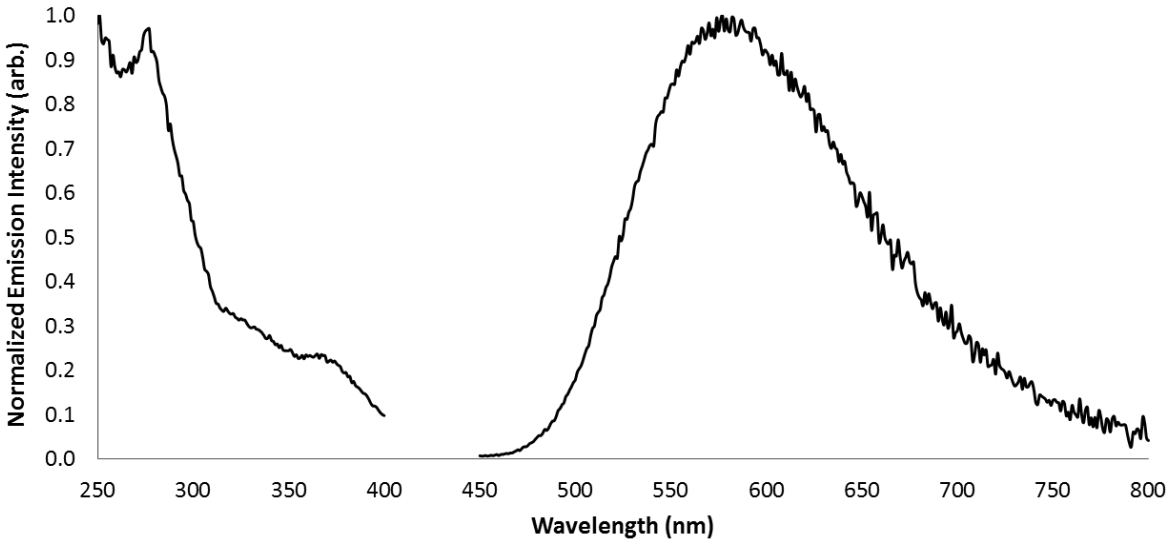


**Figure S4**. Normalised excitation and emission of **2** ($10^{-5}$ M) in $H_2O$:DMSO (99:1).

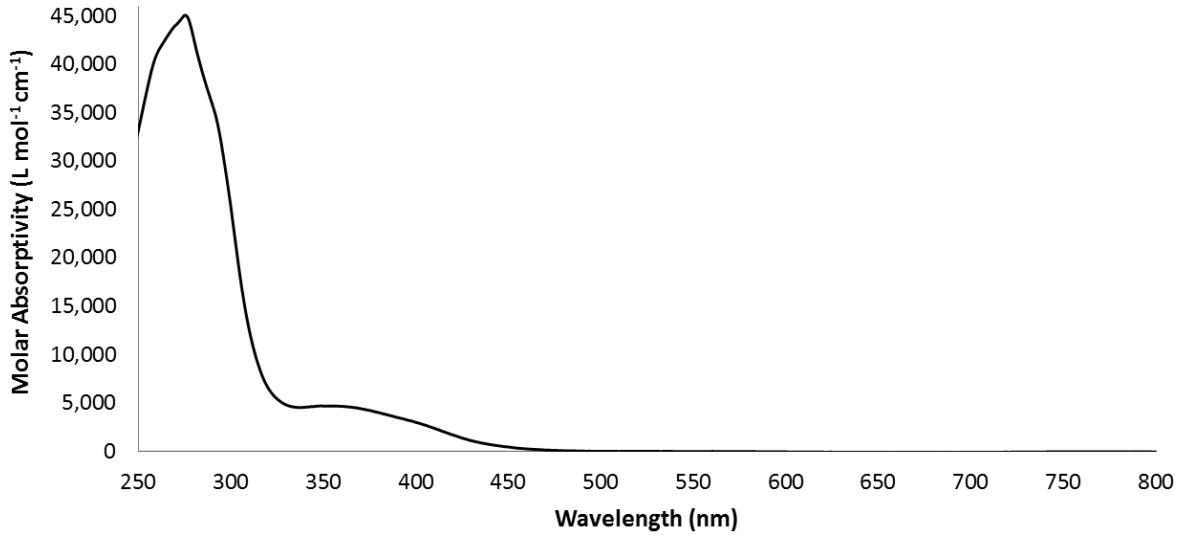


**Figure S5**. Absorption of **1** ($10^{-5}$ M) in DCM.

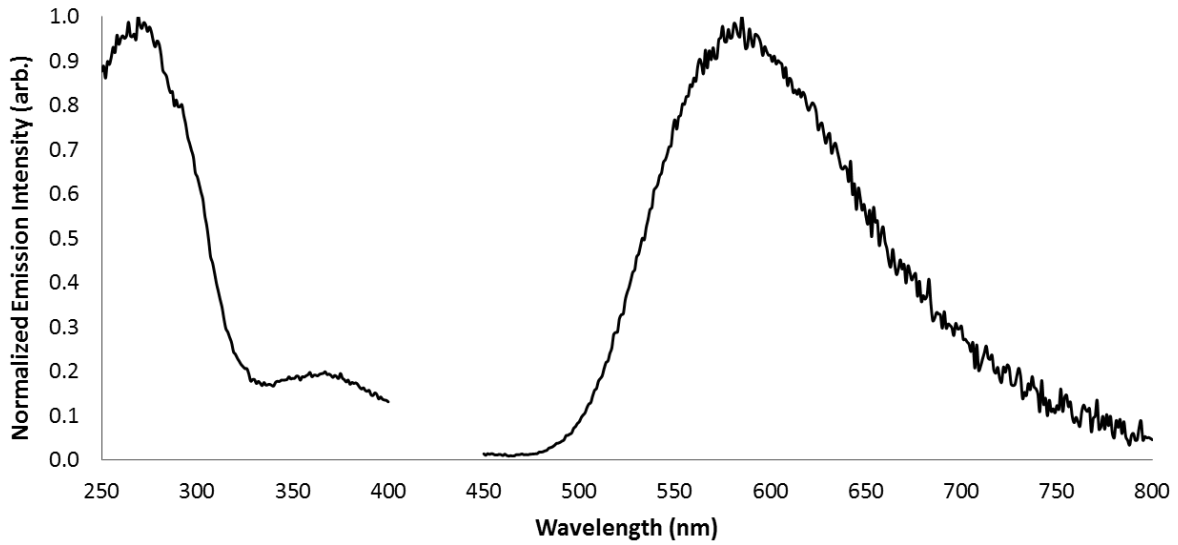


**Figure S6**. Normalised excitation and emission of **1** ($10^{-5}$ M) in DCM.

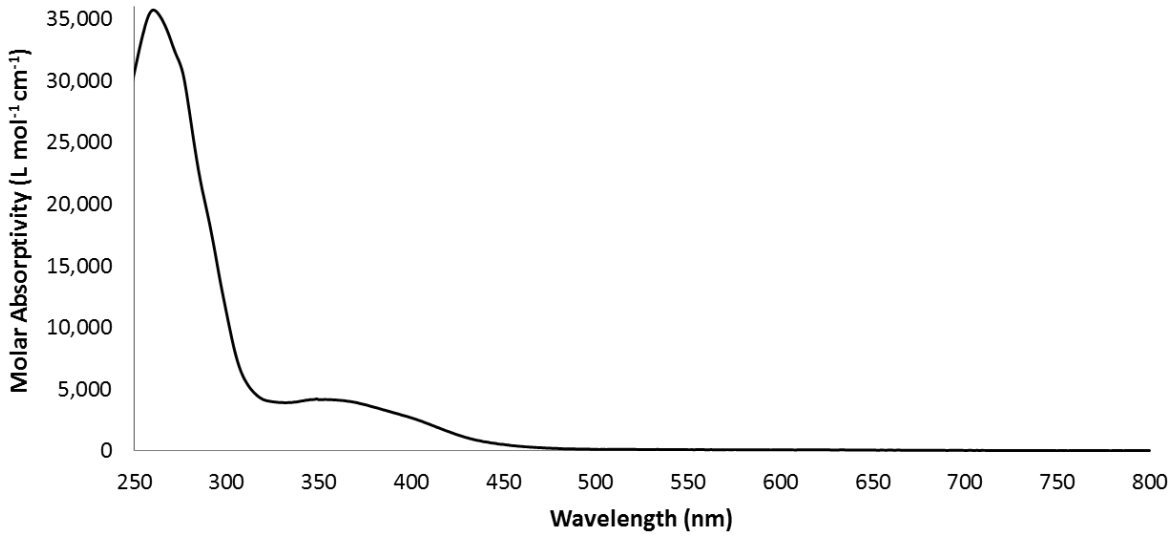


**Figure S7**. Absorption of **2** ($10^{-5}$ M) in DCM.

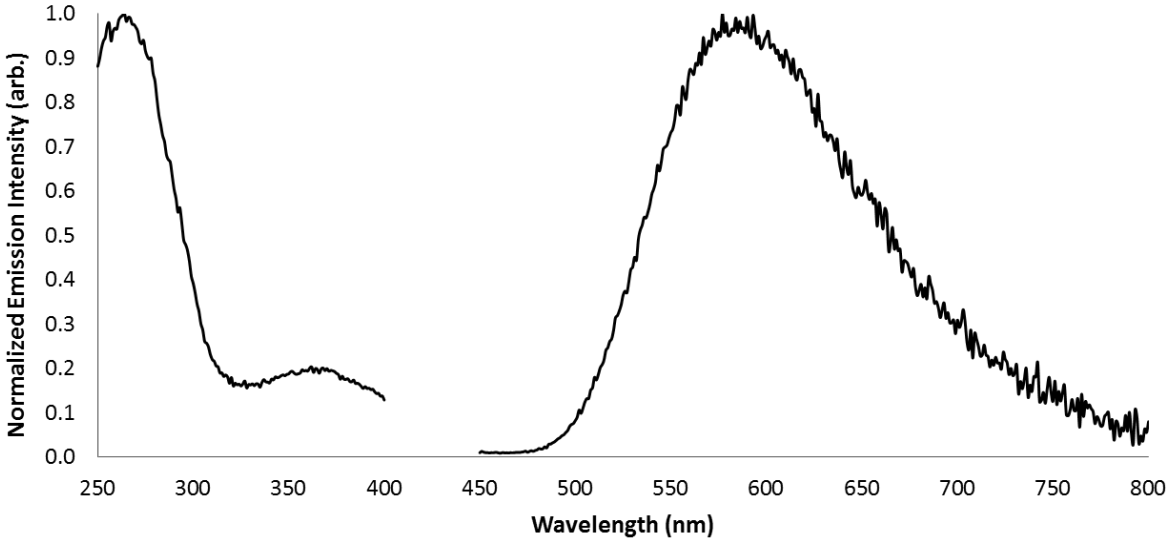


**Figure S8**. Normalised excitation and emission of **2** ($10^{-5}$ M) in DCM.

## Cellular Labelling and Visualization

### Fly stocks and cultured cells

*Drosophila* wild-type stock $w^{1118}$ was obtained from the Bloomington *Drosophila* Stock Center (Indiana University, IN, USA). Stocks were maintained on standard medium at 25˚C. Differentiated murine adipose 3T3-L1 cells were kindly provided by Dr Y. Khew-Goodall (SA Pathology, Adelaide, Australia). 3T3-L1 pre-adipocyte cells were propagated and differentiated as previously described. in Zhang et al.].[7]

### Tissue and cell and staining

Fat body tissue from *Drosophila* 3rd larval instars was dissected in 1xPBS, and immediately mounted on poly-L-lysine (Sigma, USA). Prior to staining 3T3-L1 cells were cultured for 24-48 hours to facilitate adherence on fibronectin-coated coverslips. Live tissues and cells were stained with rhenium complexes, by incubating with a 10 μM solution of each complex in 1xPBS for 10 minutes at room temperature, followed by 2-5 minutes of washing in PBS. Staining with LysoTracker®Green, MitoTracker®Red, (Invitrogen, USA), Filipin (Sigma-Aldrich, USA) and Oil Red (Sigma, USA), was performed according to manufacturer instructions. To visualise and prevent dehydration, the samples were mounted to slides with a carbomer-940 (Snowdrift farm, Tucson, USA) based optical coupling gel.[8]

### Cell imaging using two-photon and confocal microscopy

A Ziess LSM710 META NLO inverted microscope (Zeiss, Germany) was supplemented with a two-photon Mai-Tai® (tunable Ti:Sapphire femtosecond pulse laser, Spectra-Physics, Australia). The images were acquired using a Plan- APOCHROMAT 63X/ NA1.4 oil immersion

objective. Spectral fingerprinting for fat body tissue was acquired in lambda stack mode (770-860 nm continuum of excitation range, MBS 690+, spectral emission range 416-727 nm, with 38.9 nm intervals), and saved as a rhenium complex reference spectrum. Rhenium-luminescence was detected using the following setting (two-photon excitation wavelength 830 nm, beam splitter MBS 690+, emission interval 475–552 nm). For intracellular distribution studies, the rhenium complexes were excited with 830 nm two-photon laser and emission detected at either 600-654 nm (when counterstained with LysoTracker®Green) or 480-547 nm (when counterstained with MitoTracker® Red). The late endosome specific LysoTracker®Green, and mitochondria specific MitoTracker®Red (Invitrogen, USA) probes were excited using Argon 488 nm and HeNe 543 nm solid state single-photon lasers and detected in 600-654nm and 556-658nm emission intervals respectively. Cholesterol and neutral lipids were detected using Filipin and Oil Red (Sigma, USA), in tissues fixed according to manufacturer protocol. Due to highly overlapping spectra of Rhenium complex with Oil Red ($\lambda_{ex}$ = 830nm), which could not be resolved by spectral unmixing modality, the cells were stained and analysed for each dye independently. Oil Red was detected using the following settings (excitation wavelength 543 nm, beam splitter MBS 488/543, emission interval 582–754 nm). The distribution of the rhenium complexes and Filipin spectral online fingerprinting modality (Zen software, Zeiss, Germany) was used to resolve relative intracellular distribution. Phase contrast images were excited by HeNe 543 nm laser and signal collected using the T-PMP detector (Zeiss LSM710, Germany).

**Table S3.** Imaging parameters for assessing the intracellular localisation of the rhenium complexes.

| **Parameters** | **Endosome/Lysosome** | | **Mitochondria** | | **Cholesterol** | | **Lipid Droplet** | | |
|---|---|---|---|---|---|---|---|---|---|
| **Probes** | Re | LysoTrackerGreen® | Re | MitoTrackerRed® | Re | Filipin | Re | Oil Red | Phase contrast |
| **Excitation λ (nm)** | 2P 830 | 488 | 2P 830 | 543 | 2P 830 | 2P 830 | 2P 830 | 543 | 543 |
| **Detection λ (nm)** | 600-654 | 497-558 | 480-550 | 556-658 | 416-272 | 416-727 | 600-654 | 582-754 | T-PMP |
| **MBS** | 690+ | 488/543/633 | 690+ | 488/543/633 | 690+ | 690+ | 690+ | 488/543 | |
| **Capture mode** | sequential | | sequential | | spectral unmixing | | independent | | |
| **Representative Image** | Figure 4 | | ESI Figure S10 | | ESI Figure S10 | | Figure 4 | | |

2P=two-photon

## Image analysis

The emission intensity of spectral lambda stacks was assessed in ImageJ (W. Rasband, National Institute of Health, Bethesda, MD) using mean grey levels in five region of interest with area of 16px. Graphs were prepared using Microsoft excel (2010). The composite figures were prepared using ImageJ (NIH, USA) and Adobe Photoshop CS4 (Adobe Systems Inc, USA) software.

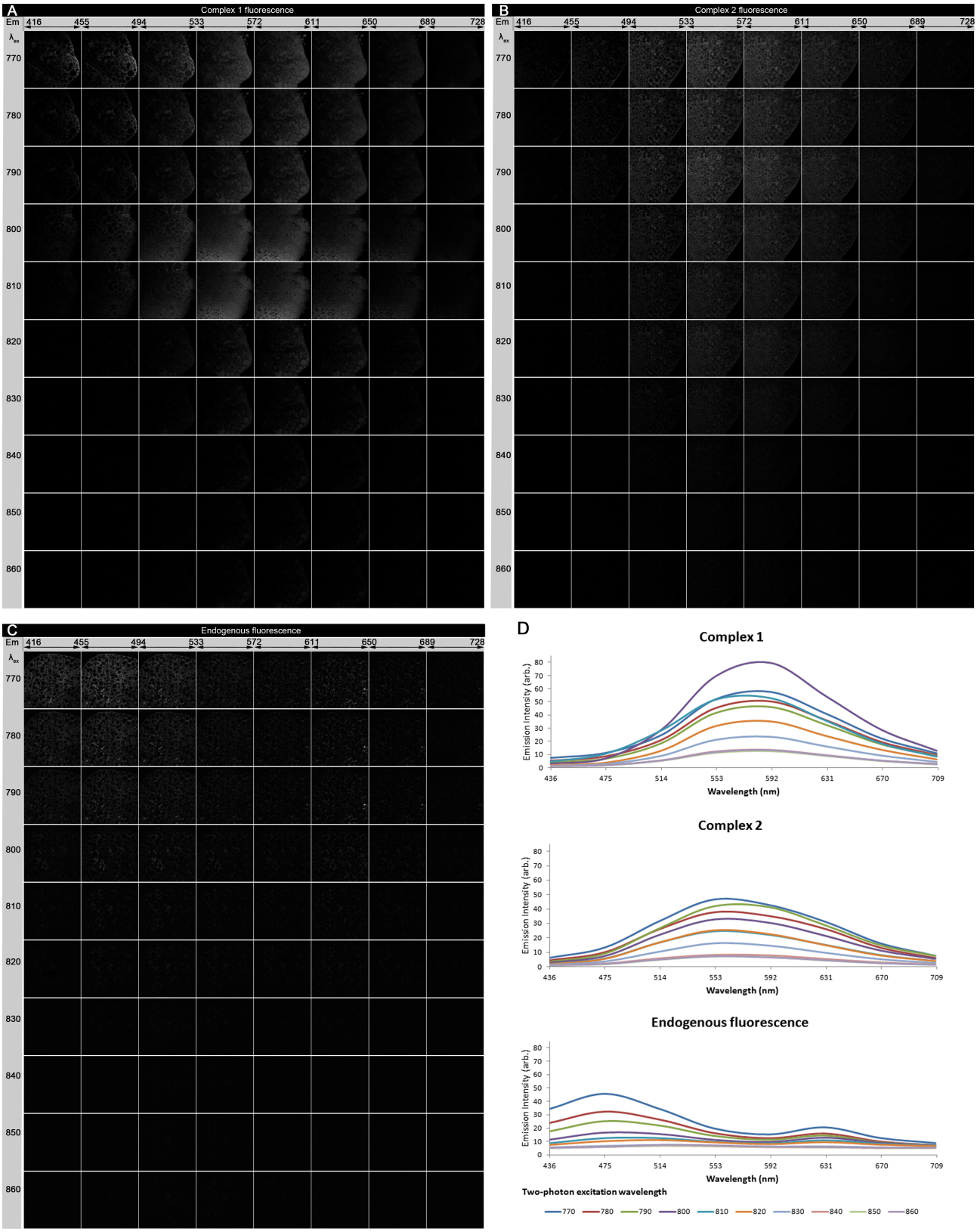


**Figure S9**. Complete spectral fingerprint of the rhenium complexes in live cells using two-photon microscopy. Representative micrographs of fat body cells acquired using the META detection module, sampling emission over the visible spectrum with 38.9 nm wavelength intervals. Fat body

cells stained with Rhenium complex **1** (A) and **2** (B), and endogenous fluorescence of fat body cells (C), which were excited with two-photon laser at the specified wavelength. Em – emission intervals in nanometers (nm). $\lambda_{ex}$ – wavelength of two-photon excitation (nm). Scale bar = 50 μm. (D) Emissions fingerprint for complex **1** (top), **2** (middle) and endogenous fluorescence (bottom).

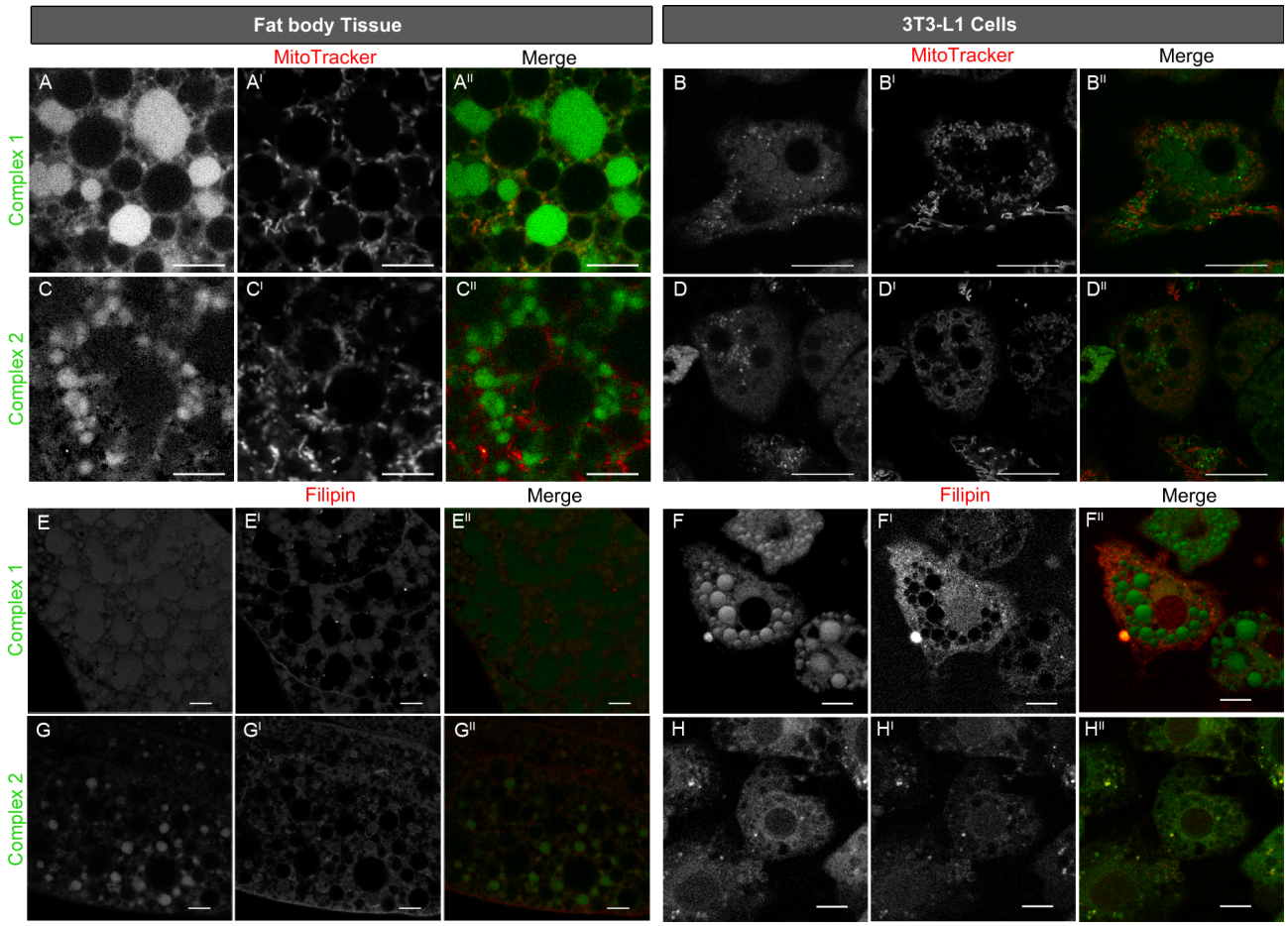


**Figure S10.** Cellular localisation of **1** and **2** visualised by two-photon excitation in *Drosophila* fat body and 3T3-L1 cells in relation to mitochondria and free cholesterol. Micrographs showing cells stained with **1** (greyscale in A, B, E and F; green in $A^{II}$, $B^{II}$, $E^{II}$ and $F^{II}$) or **2** (greyscale in C, D, G and H; green in $C^{II}$, $D^{II}$, $G^{II}$ and $H^{II}$). Mitochondria were depicted by staining with MitoTracker®Red (greyscale in $A^{I}$, $B^{I}$, $C^{I}$ and $D^{I}$; red in $A^{II}$, $B^{II}$, $C^{II}$ and $D^{II}$). Free cellular cholesterol detected by staining of fixed cells with Filipin (greyscale in $E^{I}$, $F^{I}$, $G^{I}$ and $H^{I}$;

red in $E^{II}$, $F^{II}$, $G^{II}$ and $H^{II}$). Neither **1** nor **2** showed co-localisation with MitoTracker, 2 shows some localisation with Filipin. Scale bar = 10 μm

**Attempted Time-Gated Imaging**

**Staining procedure**

The complexes were added to a MCF10A breast cancer cell culture from stock solution in DMSO at a concentration of 2000 μM. Using these conditions the final concentration of the complexes in the cell culture was 50 μM. The cells were incubated for 30 minutes. Prior to imaging, the cells were washed 4 times using Hanks Balanced Salts Solution (HBSS) to reduce the amounts of cellular precipitate. HBSS was added to cells during imaging instead of medium to avoid auto fluorescence signal from medium component. The cells were cultured in DMEM/F12 cell medium (Invitrogen, Australia), 10% Fetal Calf Serum (Invitrogen, Australia), and antibiotics with ca. 5000-10,000 cells/mL under standard culture conditions at 37 °C for 24 hours in 24-well, flat bottomed microtiter plates (Sarstedt, Germany).

**Imaging conditions**

Excitation = 405 nm

Objective x 20

Time Gated laser system settings:

Power: Maximum (~500 mW)

Gate: 20 ns

Laser On Time: 12.5 μs

Exposure Time: 12.5μs

Read Delay: ~40 ms

Camera settings

Accumulations: 2000

Shift speed: 3.7 μs

Vertical clock voltage: +2

Readout rate: 27 or 35 MHz

Pre Gain: x4

EM Gain: 140

Emission 585nm(± 15 nm)

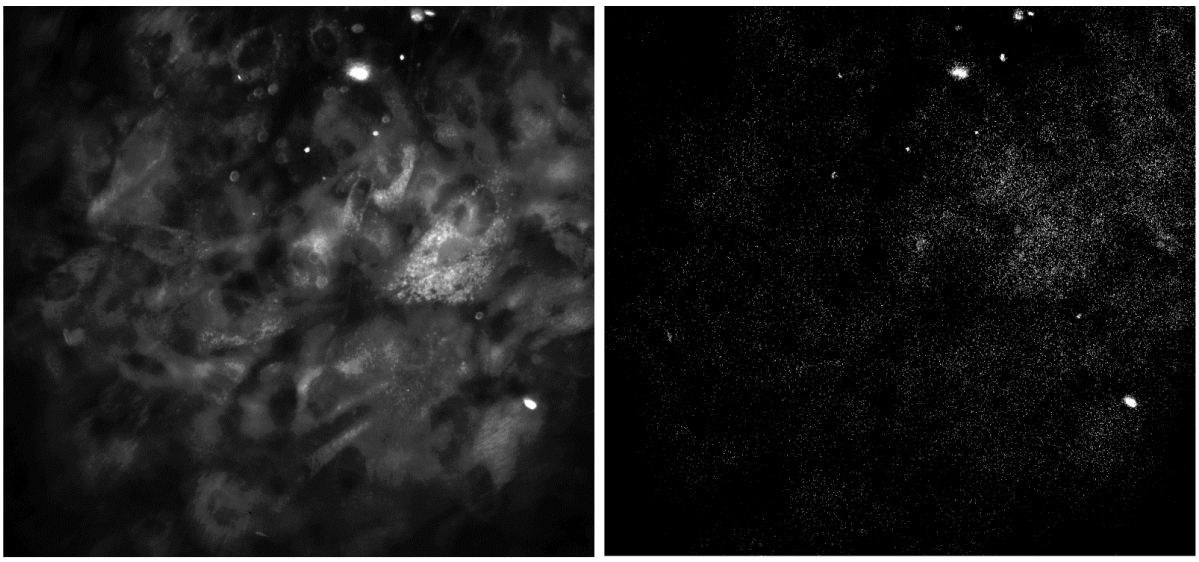

**Figure S11**. MCF10A cells stained with **1**. Imaged acquired in continuous mode (left) or time-gated mode (right).

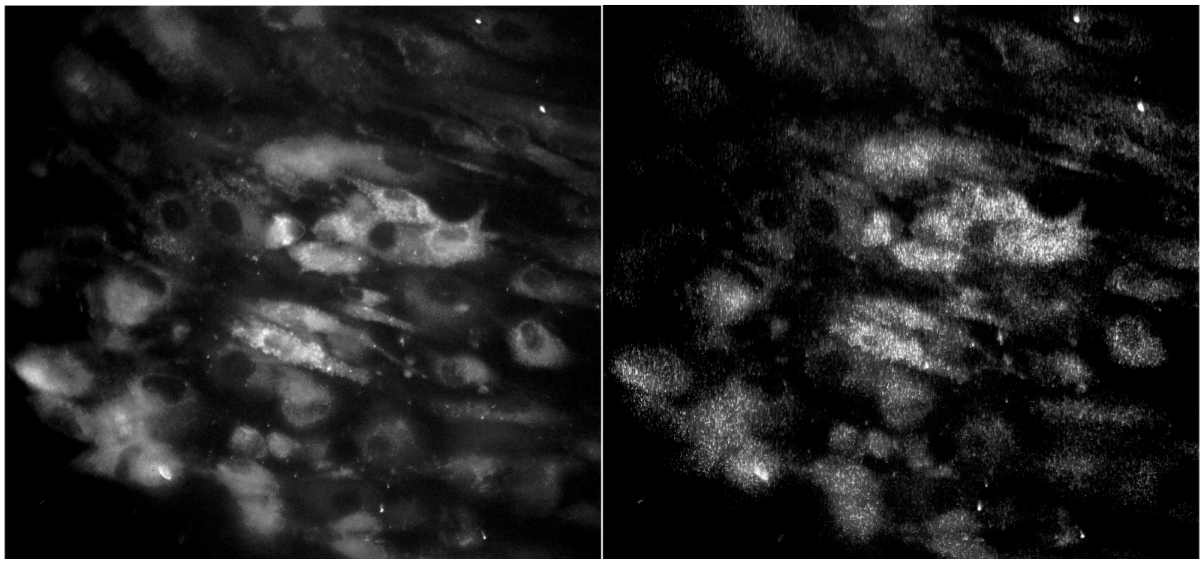

**Figure S12**. MCF10A cells stained with **2**. Imaged acquired in continuous mode (left) or time-gated mode (right).

In an attempt to identify whether the complexes were suitable for time-gated imaging, we performed the imaging experiments as previously described. Excitation at 405 nm causes strong diffuse cytoplasmic emission for for cells stained with both complexes, as shown in Figure S11 and

S12, left panels. We have ascribed the origin of this diffuse emission as fluorescence from endogenous species containing flavine-type groups. On the other hand, the time-gated emission shown in the left panels of Figure S10 and S11 highlight more localised emission in agreement with the co-localisation studies.

**MTS Assay**

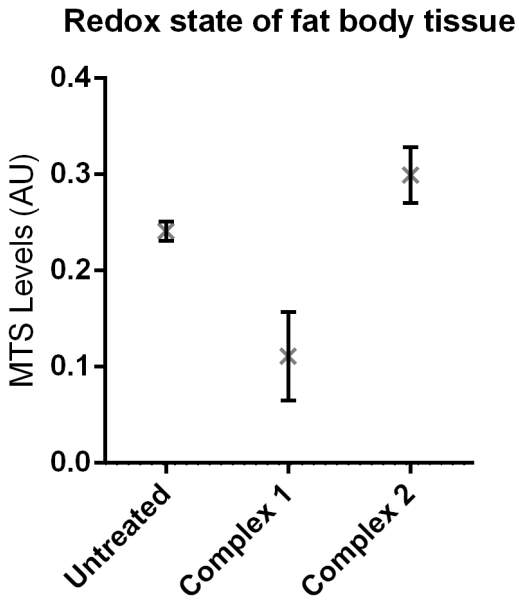


To assess cytotoxicity of the complexes, cellular NAD(P)H-dependent redox activity was measured using CellTiter 96® AQueous Non-Radioactive Cell Proliferation Assay (MTS) according to the manufacturer instruction (Promega, USA). Briefly, fat body tissues were dissected from wild-type larvae in PBS. Tissue was then incubated with 20 μM of **1** or **2** for fifteen minutes**,** then immediately transferred to 120 μL of MTS and PMS in DMEM medium in 96 well plate. The tissues were allowed to incubate at room temperature for 3 hours. The absorbance was then measured at 490 nm by VICTOR X™ Multilabel Plate Readers (PerkinElmer, MA, USA). No significant difference could be detected in the redox state of tissues treated with the complexes compared to untreated controls at the concentrations optimal for imaging. Data represent the mean ± SEM of three biological replicates for each treatment group.

**Stability Studies**

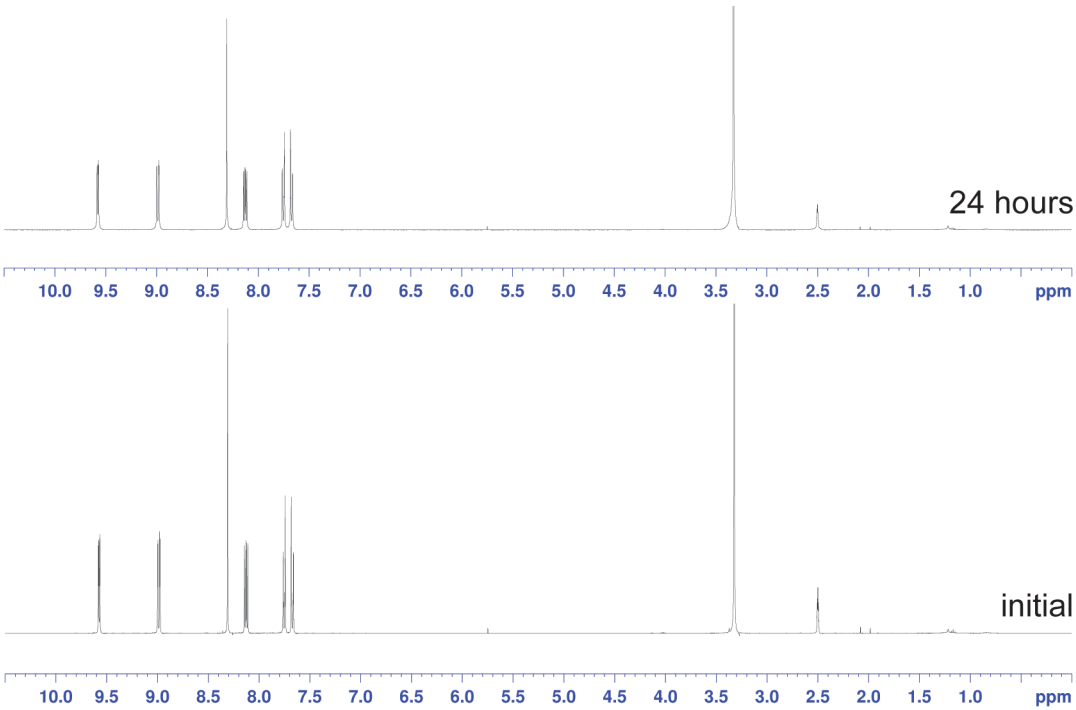


**Figure S13.** $^{1}$H-NMR spectra of **1** in $d_6$-DMSO measured within 24 hours.

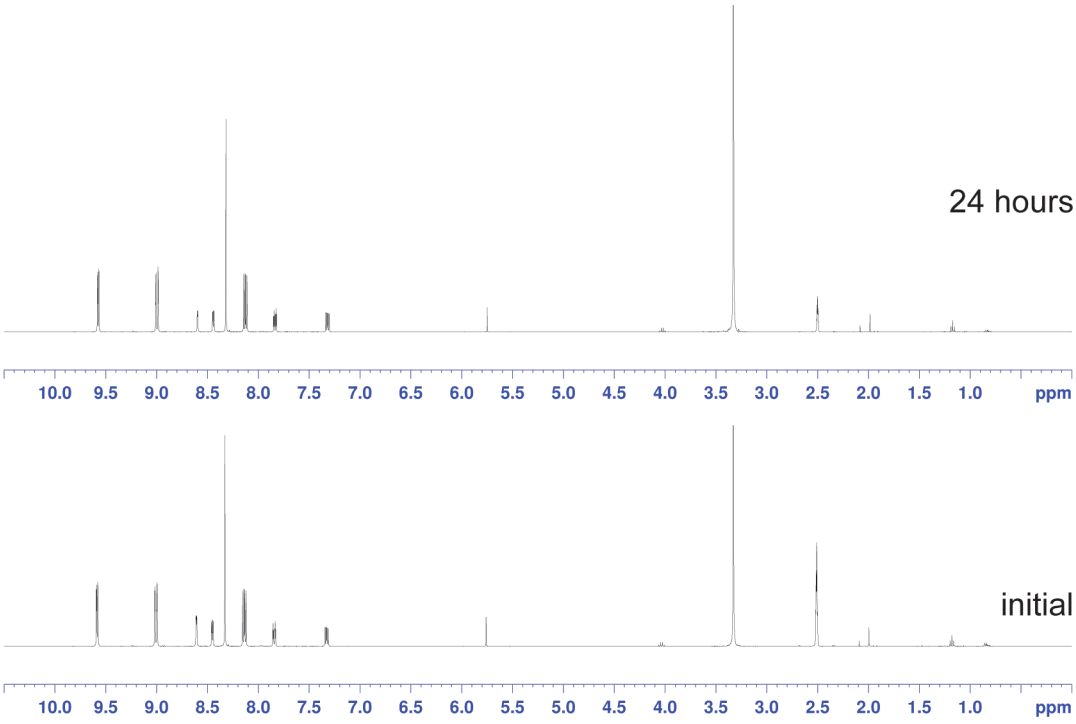


**Figure S14.** $^{1}$H-NMR spectra of **2** in $d_6$-DMSO measured within 24 hours.

## References


1. P. J. Wright, S. Muzzioli, M. V. Werrett, P. Raiteri, B. W. Skelton, D. S. Silvester, S. Stagni, and M. Massi, *Organometallics*, 2012, **31**, 7566–7578.
2. J. Demas and G. Crosby, *J. Phys. Chem.*, 1971, **75**, 991–1024.
3. J. R. Lakowicz, *Principles of fluorescence spectroscopy*, Springer, Baltimore, Third Ed., 2009.
4. M. V. Werrett, D. Chartrand, J. D. Gale, G. S. Hanan, J. G. MacLellan, M. Massi, S. Muzzioli, P. Raiteri, B. W. Skelton, M. Silberstein, and S. Stagni, *Inorg. Chem.*, 2011, **50**, 1229–1241.
5. K. Koguro, T. Oga, S. Mitsui, and R. Orita, *Synthesis*, 1998, 910–914.
6. G. M. Sheldrick, *Acta Cryst. A*, 2008, **64**, 112–122.
7. Y. Y. Zhang, X. Li, S. W. Qian, L. Guo, H. Y. Huang, Q. He, Y. Liu, C. G. Ma, and Q. Q. Tang, *Mol. Biol. Cell.*, 2011, **22**, 2165-2174.
8. E. C. Rothstein, M. Nauman, S. Chesnick, and R. S. Balaban, *J. Micros.*, 2006, **222**, 58-64.